The interaction of bacterial magnetosomes and human liver cancer cells *in vitro*

Pingping Wang[a],*, Chuanfang Chen[a], Changyou Chen[a,b], Yue Li[a], Weidong Pan[a], Tao Song[a]

[a] Beijing Key Laboratory of Bioelectromagnetism, Institute of Electrical Engineering, Chinese Academy of Sciences, Beijing 100190, PR China
[b] University of Chinese Academy of Sciences, Beijing 100049, PR China

ABSTRACT

As the biogenic magnetic nanomaterial, bacterial magnetic nanoparticles, namely magnetosomes, provide many advantages for potential biomedical applications. As such, interactions among magnetosomes and target cells should be elucidated to develop their bioapplications and evaluate their biocompatibilities. In this study, the interaction of magnetosomes and human liver cancer HepG2 cells was examined. Prussian blue staining revealed numerous stained particles in or on the cells. Intracellular iron concentrations, measured through inductively coupled plasma optical emission spectroscopy, increased with the increasing concentration of the magnetosomes. Transmission electron microscopy images showed that magnetosomes could be internalized in cells, mainly encapsulated in membrane vesicles, such as endosomes and lysosomes, and partly found as free particles in the cytosol. Some of the magnetosomes on cellular surfaces were encapsulated through cell membrane ruffling, which is the initiating process of endocytosis. Applying low temperature treatment and using specific endocytic inhibitors, we validated that macropinocytosis and clathrin-mediated endocytosis were involved in magnetosome uptake by HepG2 cells. Consequently, we revealed the interaction and intrinsic endocytic mechanisms of magnetosomes and HepG2 cells. This study provides a basis for the further research on bacterial magnetosome applications in liver diseases.

1. Introduction

Bacterial magnetosomes, a type of biologically synthesized magnetic nanoparticles, have numerous advantages, such as homogeneity, biocompatibility and suitable surface properties [1–4] that make them a good candidate for many biomedical and pharmaceutical applications, such as tumor hyperthermia, drug delivery, biomedical imaging and bioseparation [5–8].

The intrinsic mechanisms of interactions between nanoparticles and target bio-organisms at a cellular level should be elucidated to evaluate the biocompatibility of nanoparticles and develop their biomedical applications. Nanomaterials possess unique physical, chemical and biological properties that greatly differ from their bulk materials because nanomaterials are extremely small [9]. The interaction of nanoparticles with cells and biological tissues is closely related to various nanoparticle properties, such as particle size, shape, coating, surface charge and composition [10–12]. Cell type, state and cellular environment can also affect cell-nanoparticle interactions [13–16]. Therefore, the inherent interaction of magnetosomes and target cells should be carefully addressed because of the unique particle properties

of bacterial magnetosomes, such as biomembrane coating, to improve their bioapplications and evaluate their biocompatibilities.

The most direct interacting pathway of nanoparticles and cells is the active endocytosis, rather than simple passive permeation [17,18]. Endocytosis is an active and energy-dependent cellular process by which extracellular substances are engulfed. This process depends on dynamic cell membrane deformation processes, such as ruffling and budding. Wrapped vesicles are pinched off from the plasma membrane and then transported to target organelles to internalize particles and macromolecules [17].

Several endocytic mechanisms are involved in the uptake of extracellular materials, including nanoparticles. Endocytosis is classified into two common mechanisms on the basis of cargo size: phagocytosis or cell eating and pinocytosis or cell drinking. Phagocytosis is primarily responsible for the uptake of large particles (size > 0.5 μm), such as bacteria, cell debris and apoptotic cells. This process is typically carried out by only few professional phagocytes. Pinocytosis is ubiquitous to almost all eukaryotic cells and mainly considered as a means of taking up fluid surrounding the cell surface and the subsequent internalization of the solutes [19]. Pinocytosis is

---

further divided into several classes, including macropinocytosis, clathrin-mediated endocytosis (CME), the caveolae-mediated endocytosis and other clathrin- and caveolae-independent endocytic pathways [20,21]. However, the underlying endocytic mechanisms of bacterial magnetosomes still remain unclear.

Several kinds of nanoparticles can accumulate in liver tissues; as such, these particles are promising drug carrier targeting liver tumours [22,23]. Nevertheless, whether bacterial magnetosomes can interact with liver cancer cells has yet to be fully elucidated. Therefore, this study examined the interaction and intrinsic mechanism of bacterial magnetosomes and human live cancer HepG2 cells.

2. Materials and methods

2.1. AMB-1 culture and magnetosome extraction

Magnetospirillum magneticum AMB-1 (ATCC 700264, Manassas, VA, USA) was cultured in accordance with previously described methods [24] to extract bacterial magnetosomes. AMB-1 cells were grown microaerobically in enriched *Magnetospirillum* growth medium in the dark at 28 ± 1 °C, harvested through centrifugation at $5000 \times g$ for 10 min and re-suspended in 0.1 M phosphate buffer saline (1×PBS, pH 7.4). The bacterial cells were then fragmented through ultrasonication (180 W, 4 s work, 4 s interval, 99 repetitions) thrice by using an ultrasonic apparatus (Ningbo Xinzhi Biotechnology, Zhejiang, China). Bacterial magnetosomes were extracted from the solutions by utilizing an NdFeB magnet (50 mm×50 mm×25 mm, with a magnetic flux density of approximately 0.2 T at the surface centre; Shenyang General Magnetic Co., Ltd., Shenyang, China). The extracted magnetosomes were initially washed with 1×PBS thrice and then with ddH$_2$O thrice. Afterward, the extracted magnetosomes were resuspended with ddH$_2$O at a stocking concentration of 10 mg/mL, sterilized by autoclaving and stored at 4 °C.

2.2. Measurement of the magnetic hysteresis loop of the purified magnetosomes

For the purified magnetosome sample, approximately 20 μL of magnetosome suspension was deposited and dried on the surface of a small nonmagnetic cover slide (0.22×0.22 cm) in the presence of a strong magnetic field (approximately 2 T produced by a laboratory-made electromagnetic equipment). The magnetic hysteresis loop of the magnetosomes was detected by using a Model 3900 vibrating sample magnetometer (Princeton Measurements Corporation VSM 3900, Princeton, NJ, USA).

2.3. Cell culture and treatments

Liver hepatocellular carcinoma cell line HepG2 (No. 3111C0001CCC000035; China Infrastructure of Cell Line Resources, Beijing, China) was maintained in Dulbecco's modified Eagle's medium (DMEM, Gibco/Life Technologies, Grand Island, NY, USA) supplemented with 10% fetal bovine serum (Australian origin, Hyclone Laboratories, Logan, UT, USA), 100 IU/mL penicillin (Sigma-Aldrich, St Louis, MO, USA) and 100 μg/mL streptomycin (Sigma-Aldrich) at 37 °C in 5% CO$_2$. HepG2 cells were seeded with an appropriate density in cell culture medium and incubated for 24 h. The medium was then replaced with the magnetosome working solution for the succeeding experiments. The magnetosome stocking solution (10 mg/mL) was dispersed sufficiently through sonication at 40 kH, 300 W for at least 5 min in a water bath (Ningbo Xinzhi Biotechnology) just before incubation with the cultured cells.

For low-temperature treatment, the cells were pre-incubated at 4 °C for 10 min, treated with 0, 100, 200 and 400 μg/mL magnetosomes and incubated respectively at 4 °C and 37 °C for another 3 h. For endocytosis inhibitor treatment, HepG2 cells were pretreated with different inhibitors in the cell culture media, and the media were replaced with magnetosome working solutions. The pretreated concentration and period of each inhibitor were as follows: 10 μg/mL cytochalasin B preteated for 2 h; 2 μM rottlerin pretreated for 30 min; 200 μM monodansyl cadaverine (MDC) pretreated 15 min; and 50 μg/mL nystatin preteated 15 min. All the inhibitors were obtained from Sigma-Aldrich.

2.4. Transmission electron microscopy (TEM)

The cells incubated with or without 100 μg/mL magnetosomes for 24 h were fixed in a suspension with 2.5% glutaraldehyde in 1×PBS for at least 1 h, dehydrated with graded ethanol and propylene oxide and embedded in Epon (SPI-Pon 812 Epoxy Embedding kit, SPI Supplies, West Chester, PA, USA). Thin sections (70 nm) were stained with uranyl acetate and lead citrate and then observed using a transmission electron microscope (H-7650, Hitachi, Tokyo, Japan). To determine the morphological characteristics of AMB-1 or isolated magnetosomes, we collected and re-suspended AMB-1 cells with 1×PBS. We diluted the extracted magnetosome solution with ddH$_2$O and prepared the sample for TEM by drying a drop of AMB-1 or magnetosome suspension on a copper grid-supported transparent carbon foil.

2.5. Prussian blue staining

Prussian blue staining kit (Beijing Solarbio Science & Technolgy, Beijing, China) was applied to detect iron, and experiments were conducted according to the manufacturer's instruction. In Brief, HepG2 cells treated with magnetosomes were washed with 1×PBS thrice to remove the free particles and then fixed with 4% paraformaldehyde. The magnetosomes interacting with the cells were stained with Prussian blue staining solution, and the cytoplasm was stained with eosin solution. The cells were subsequently observed under an inverted optical microscope system (Olympus, Tokyo, Japan), and cellular images were captured.

2.6. Inductively coupled plasma optical emission spectrometry (ICP-OES)

Intracellular iron concentration was quantified through inductively coupled plasma optical emission spectrometry (ICP-OES) (iCAP 6300, Thermo Scientific, MA, USA). HepG2 cells were treated with 0, 50, 100, 200 and 400 μg/mL magnetosomes for 24 h and washed with 1×PBS thrice to remove the free magnetosomes. The cells were digested with trypsin, counted, harvested through centrifugation and washed with 1×PBS twice. The supernatants were then removed. The cell samples were dissolved completely with concentrated nitric acid (65–68%) and heated for 4 h at 85 °C. After the concentrated nitric acid evaporated, the samples were diluted with 1% nitric acid to obtain the final volume of 5 mL. The iron concentration was determined from standard solutions with known concentrations. The statistical data of iron concentrations were expressed as mean ± standard deviation. The experiments were repeated thrice.

3. Results and discussion

3.1. Characterization of magnetotactic bacteria and magnetosomes

TEM were conducted to observe the morphological characteristics of bacterial magnetosomes directly. In Fig. 1A and B, a kind of magnetotactic bacteria, *Magnetospirillum magneticum* AMB-1 contained the endogenous magnetosomes arranged in chains along the long axis of the cell body. The TEM images of the extracted magnetosomes showed that the particles exhibited good dispersion and did not aggregate together severely (Fig. 1C and D). The magnetosomes were also surrounded by a 2–3 nm thick membrane, which was not
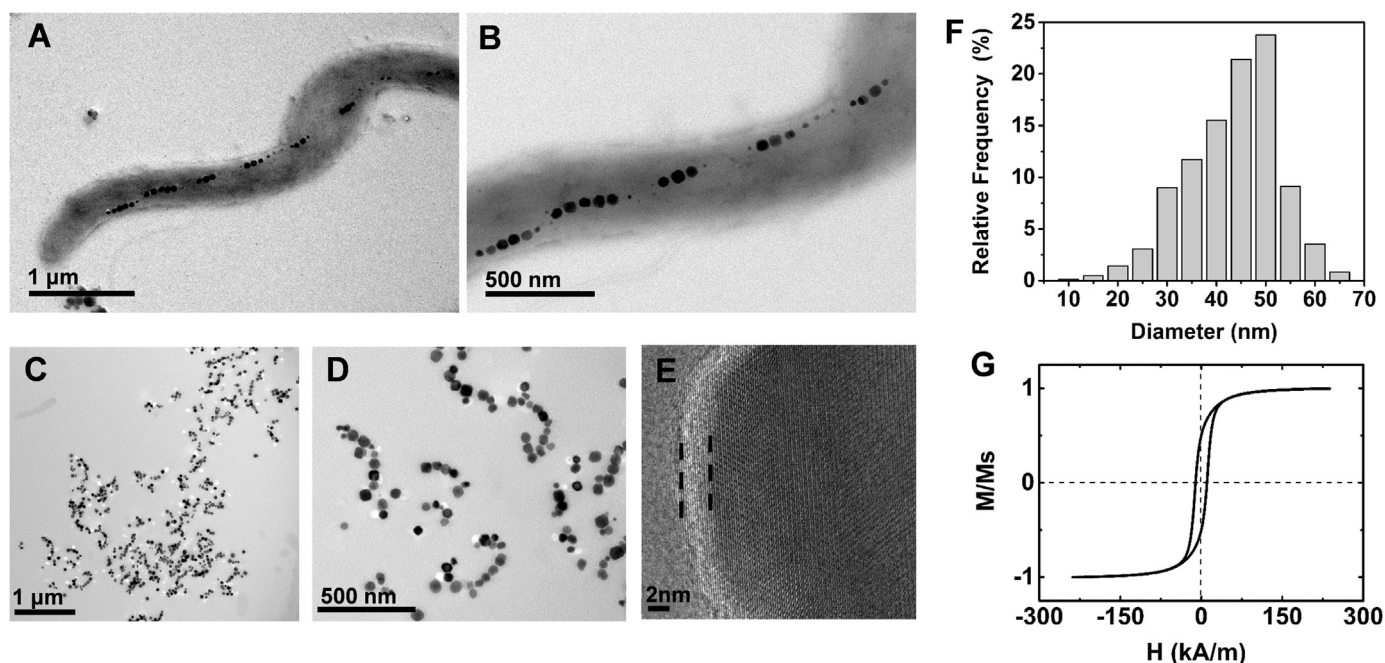
Fig. 1. Characterization of magnetotactic bacterium AMB-1 and magnetosomes. (A) and (B) TEM images of AMB-1 with different magnifications. (C)–(E) TEM images of the extracted magnetosomes with different magnifications. The double dashed lines in (E) showed the magnetosome membrane with a thickness of approximately 2–3 nm. (F) Size distribution of magnetosomes (n=845). (G) Magnetic hysteresis loop of the purified magnetosomes. M refers to the magnetization of the purified magnetosomes, M_s refers to the saturation magnetization of magnetosomes.
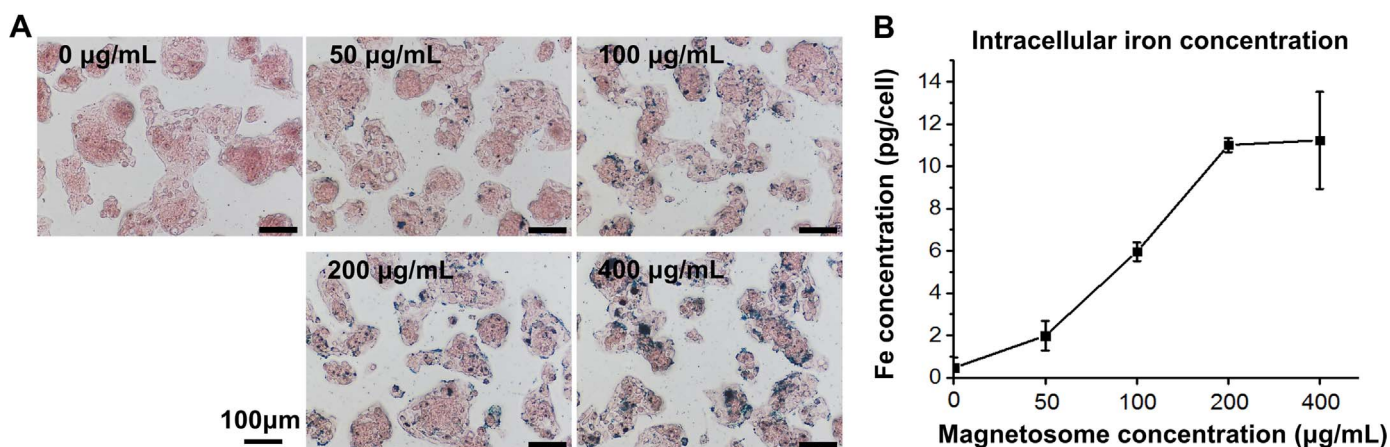

Fig. 2. Dose-dependent interaction of magnetosomes with HepG2 cells. (A) Prussian blue staining of HepG2 cells treated with 0, 50, 100, 200 and 400 µg/mL magnetosomes for 6 h. (B) Intracellular iron concentrations of cells treated with 0, 50, 100, 200 and 400 µg/mL magnetosomes for 24 h. n =3. (For interpretation of the references to color in this figure legend, the reader is referred to the web version of this article.)

destroyed during extraction through ultrasonication. The membrane wrapping provides magnetosome particles a natural surface coating and ensures particle stability and biocompatibility [4,25]. The particle size distribution of magnetosomes was analyzed on the basis of the TEM images. The average size of magnetosomes in AMB-1 was approximately 41 nm, and the frequency of the large particles (> 50 nm) decreased greatly (Fig. 1F). This finding suggested that mature magnetosomes displayed good homogeneity.

The magnetic hysteresis loop of the purified magnetosomes was measured (Fig. 1G), and the following results were obtained. The coercive force H_c was approximately 12.9 kA/m and the ratio of remnant magnetization (Mr) to saturation magnetization (Ms) was 0.52, which indicated that the endogenous magnetosomes inside AMB-1 cells were magnetic single-domain particles. Actually, the chain-like alignment of the bacterial magnetic nanoparticles provides the magnetosome chain a large magnetic moment, ensures magnetotactic bacterial cell sensing and responding to external magnetic fields, including

weak magnetic field, such as geomagnetic field [1,26].

3.2. Dose-dependent interaction of magnetosomes with HepG2 cells

To evaluate the interaction of the extracted magnetosomes and liver cancer cells, we treated the HepG2 cells with different magnetosome concentrations. Magnetosomes are mainly composed of Fe_3O_4, Fe_3S_4 [27], iron ion can react with Prussian blue and appear blue. After HepG2 cells were incubated with different magnetosome concentrations for 6 h, Prussian blue staining revealed stained dots in or on HepG2 cells (Fig. 2A). This finding demonstrated that magnetosomes can bind to the cultured cells. Moreover, the amounts of the blue dots increased as the magnetosome-concentrations increased (Fig. 2A). ICP-OES was performed to detect the intracellular iron concentrations after magnetosome was administrated at different concentrations for 24 h. Consistently, the results showed that the intracellular iron concentrations increased in a magnetosome-dose-dependent manner
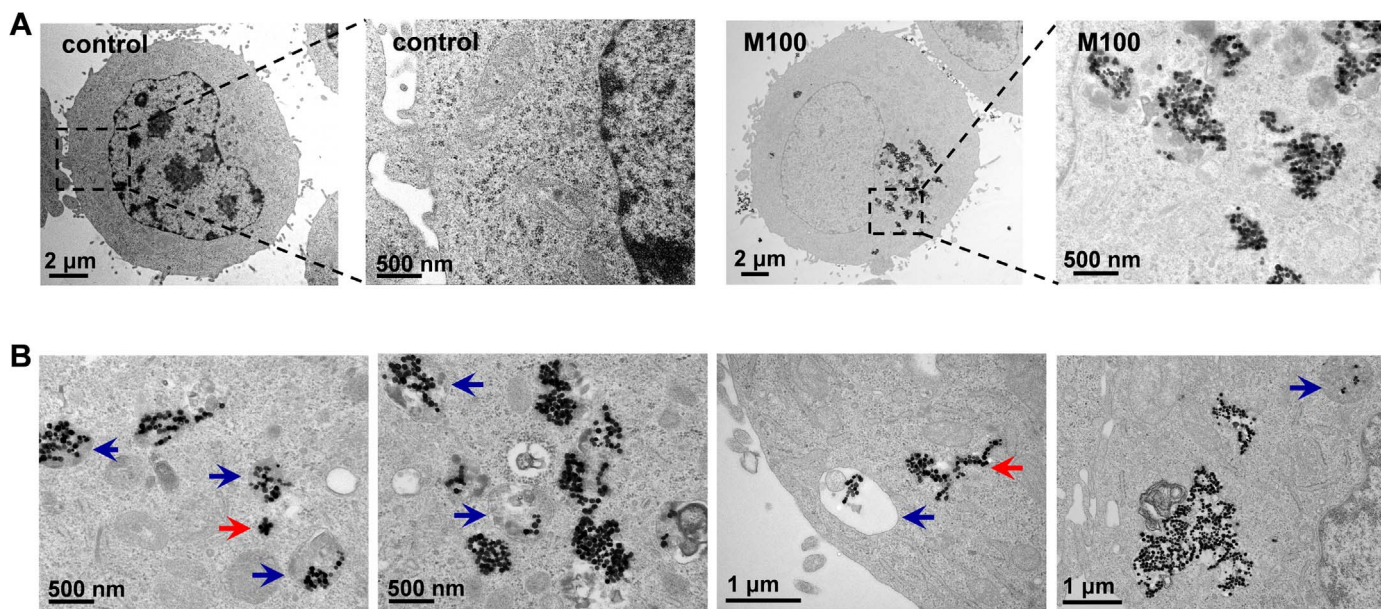
Fig. 3. TEM images of magnetosome-treated and untreated HepG2 cells. (A) Morphology of untreated control cells and 100 μg/mL magnetosome-treated cells for 24 h. (B) TEM images of the ultrastructures of 100 μg/mL magnetosome-treated cells and the different subcellular localizations of magnetosomes. Blue arrows indicate the magnetosomes wrapped in membrane vesicles. Red arrows show the freely dispersed magnetosomes. (For interpretation of the references to color in this figure legend, the reader is referred to the web version of this article.)
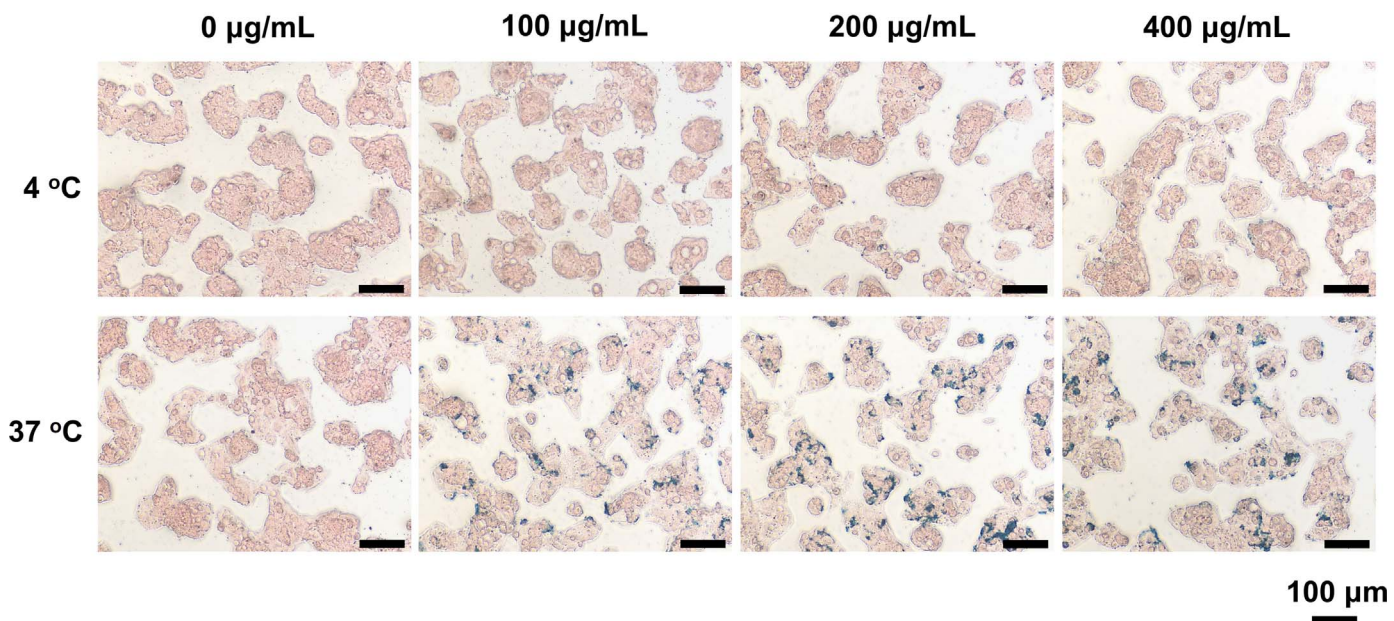

Fig. 4. Prussian blue staining of HepG2 cells incubated with magnetosomes at different temperatures. HepG2 cells preincubated at 4 °C for 10 min were treated with 0, 100, 200 and 400 μg/mL magnetosomes incubated at 4 °C and 37 °C for another 3 h respectively. (For interpretation of the references to color in this figure legend, the reader is referred to the web version of this article.)

and became nearly saturated at 400 μg/mL (Fig. 2B).

3.3. Internalization of magnetosomes in HepG2 cells and intracellular localizations of particles

In order to further identify whether magnetosomes can enter cellular bodies or merely attach or adhere to cellular surfaces, we performed TEM and observed the cellular ultrastructures. The results showed that magnetosomes could be taken up by HepG2 cells (Fig. 3A). A majority of the internalized magnetosomes were mainly encapsulated in monolayer membrane vesicles (Fig. 3B, blue arrows), which were commonly recognized as classical endosomes and lysosomes. The size of these vesicles wrapping the internalized magnetosomes ranged from

0.25μm to 2 μm in diameter. A minority of magnetosomes located freely in the cytosol (Fig. 3B, red arrows). These magnetosomes may be produced when they escape from lysosomes or permeate the cytosol through direct transduction across the plasma membrane [18].

3.4. Endocytosis-dependent cellular uptake of magnetosomes

The membrane vesicle encapsulation of magnetosomes, as demonstrated in the TEM images, implies that the uptake of magnetosomes is probably mediated by cellular endocytosis, which is an important mechanism to internalize extracellular substances and accompanied by cytoplasmic membrane dynamic deformation and vesicular transportation [18]. Endocytosis is an energy-consuming and temperature-
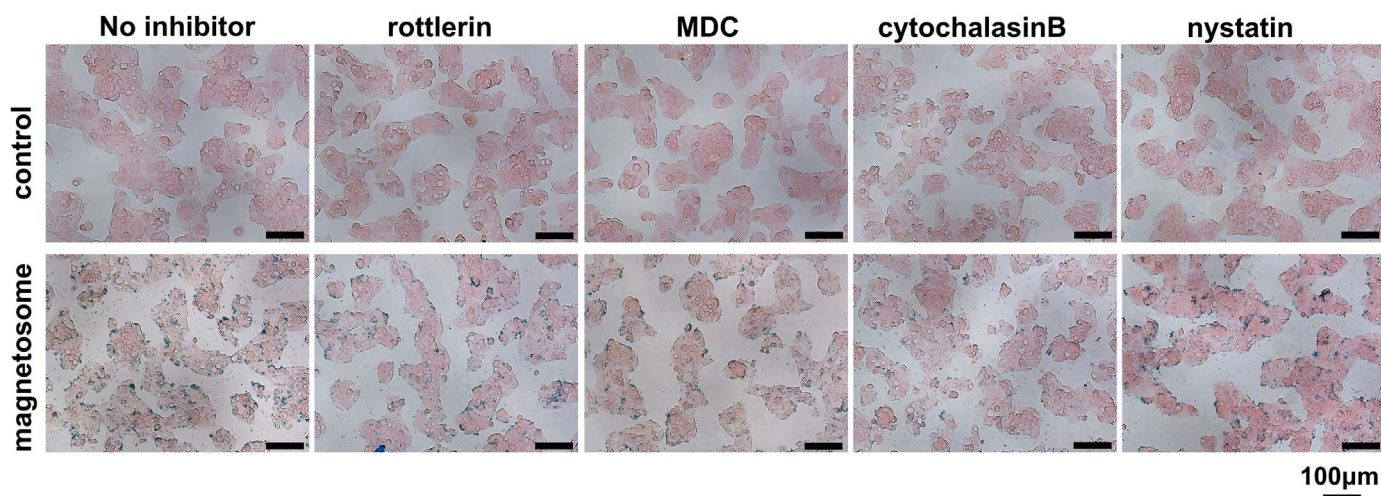
Fig. 5. Prussian blue staining of magnetosome-treated HepG2 cells with pretreatments of the inhibitors of different endocytic pathways. HepG2 cells were pretreated with the corresponding endocytic inhibitors, and 200 μg/mL magnetosomes were treated for another 4 h. The pretreatments of the endocytic inhibitors were as follows: 2 μM rottlerin pretreatment for 30 min to inhibit macropinocytosis; 200 μM monodansyl cadaverine (MDC) pretreatment for 15 min to inhibit clathrin-mediated endocytosis; 10 μg/mL cytochalasin B pretreatment for 2 h to inhibit actin dependent endocytosis; and 50 μg/mL nystatin pretreatment for 15 min to inhibit caveolae-mediated endocytosis. (For interpretation of the references to color in this figure legend, the reader is referred to the web version of this article.)
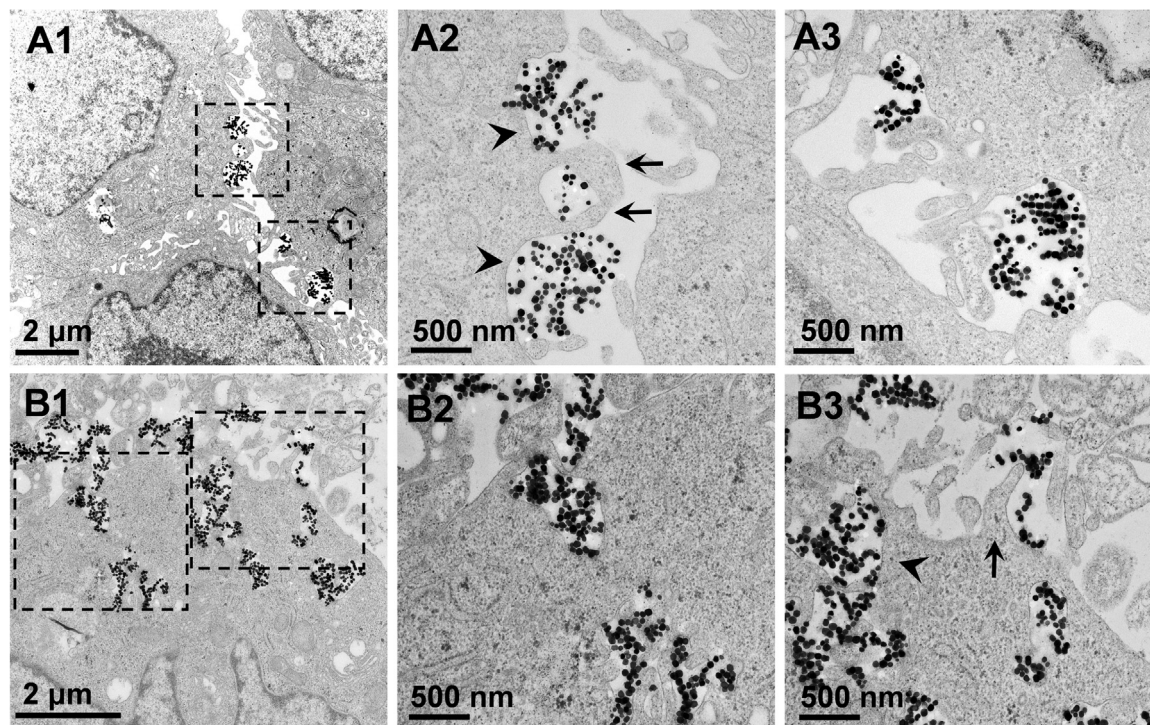

Fig. 6. Membrane encapsulation of magnetosomes on cellular surfaces. TEM images of the ultrastuctures of the surface cytoplasmic membrane. The rectangular regions in A1 and B1 were magnified and shown in A2 and A3 and B2 and B3, respectively. Arrowheads and arrows denote cell membrane invagination and evagination to encapsulate the adherent magnetosomes, respectively.

dependent active cellular process [28]. We incubated HepG2 cells with magnetosomes at 4 °C and 37 °C respectively. Compared with the control temperature (37 °C), low temperature (4 °C) significantly inhibited the interaction of magnetosomes and HepG2 cells (Fig. 4), as revealed by Prussian blue staining. This finding indicated that the uptake of magnetosomes was dependent on active endocytosis that could be influenced by low temperature.

To further distinguish the specific pathways involved in magnetosomes internalization, HepG2 cells were pretreated with the following inhibitors to suppress the endocytic pathways. The respective endocytic pathways of the inhibitors were as follows: nystatin, caveolae-mediated endocytosis inhibitor [29]; rottlerin, macropinocytosis inhibitor [30];

MDC, clathrin-mediated endocytosis inhibitor [31]; and cytochalasin B, inhibitor of actin dependent endocytosis, such as macropinocytosis and phagocytosis [21]. Prussian blue staining revealed that the positive blue-stained dots of HepG2 cells treated with 200 μg/mL magnetosome were profoundly decreased after MDC, cytochalasin B and rottlerin pretreatments were administered respectively. By constrast, the positive blue-stained dots did not decreased significantly after nystatin pretreatment was given (Fig. 5). Therefore, multiple endocytic pathways, such as macropinocytosis and clathrin-mediated endocytosis, were involved in magnetosome uptake by HepG2 cells.

Generally, macropinocytosis take up large particles and form macropinosomes with variable diameters ranging from 0.2μm to

10 μm [32]. Clathrin-mediated endocytosis always produces vesicles with a diameter of less than 300 nm, wheras the diameter of caveolae-mediated endocytosis vesicles is much smaller or commonly less than 120 nm [17,19]. Therefore, it is reasonable that macropinocytosis and clathrin-mediated endocytosis play more important roles in the cellular uptake of magnetosomes with an average diameter of approximately 50 nm. In consist, from the TEM images, size of the intracellular vesicles encapsulating magnetosomes was ranged from 250 nm to 2 μm in diameter as mentioned above.

3.5. Membrane encapsulation of magnetosomes on cellular surfaces

Membrane invagination or evagination leading to adherent nano-particle encapsulation is the initiating event of nanoparticles endocytosis [17]. We further observed the morphological characteristics of the cell surface membrane from the TEM images. It could be found that some particles on the cell surface were encapsulating by the cell membrane invagination (arrowheads in Fig. 6) and evagination (arrows in Fig. 6), which are the representative structures of endocytosis. It was further proved that magnetosomes were internalized into HepG2 cells through cell endocytosis.

4. Conclusion

Bacterial magnetosomes can bind to and interact with liver cancer HepG2 cells in a magnetosome-dose-dependent manner. Magnetosomes can internalize in cell bodies and mainly localize in membrane vesicles, such as endosomes and lysosomes. The cellular uptake of magnetosomes in HepG2 cells mainly occurs through temperature-dependent endocytosis, and this process involves multiple endocytic pathways, such as macropinocytosis and clathrin-mediated endocytosis. Thus this study demonstrated the interaction of magnetosomes and liver cancer cells, revealed the type and intrinsic mechanism of this interaction and especially identified the involved endocytic pathways. This study also promoted further research on the biocompatibility and biomedical applications of bacterial magnetosomes and provided insights into the diagnosis and therapy of liver diseases by using bacterial magnetosomes as target drug carriers, imaging contrast agents and hyperthermal materials.

References

[1] D. Schuler, J. Mol. Microbiol. Biotechnol. 1 (1999) 79–86.
[2] A.C. Araujo, F. Abreu, K.T. Silva, et al., Mar. Drugs 13 (2015) 389–430.
[3] J. Xie, K. Chen, X. Chen, Nano Res. 2 (2009) 261–278.
[4] S. Schwarz, F. Fernandes, L. Sanroman, et al., J. Magn. Magn. Mater. 321 (2009) 1533–1538.
[5] D. Schuler, R.B. Frankel, Appl. Microbiol. Biotechnol. 52 (1999) 464–473.
[6] E. Alphandery, Front. Bioeng. Biotechnol. 2 (2014) 5.
[7] Y.G. Liu, Q.L. Dai, S.B. Wang, et al., Int. J. Nanomed. 10 (2015) 1387–1397.
[8] S. Meriaux, M. Boucher, B. Marty, et al., Adv. Healthc. Mater. 4 (2015) 1076–1083.
[9] J. Tian, J. Xu, F. Zhu, et al., J. Chromatogr. A 1300 (2013) 2–16.
[10] X. Duan, Y. Li, Small 9 (2013) 1521–1532.
[11] V. Zavisova, M. Koneracka, J. Kovac, et al., J. Magn. Magn. Mater. 380 (2015) 85–89.
[12] P. Pradhan, J. Giri, R. Banerjee, et al., J. Magn. Magn. Mater. 311 (2007) 282–287.
[13] D.A. Kuhn, D. Vanhecke, B. Michen, et al., Beilstein J. Nanotechnol. 5 (2014) 1625–1636.
[14] M. Mahmoudi, J. Meng, X. Xue, et al., Biotechnol. Adv. 32 (2014) 679–692.
[15] L. Treuel, X. Jiang, G.U. Nienhaus, J. R. Soc. Interface 10 (2013) 20120939.
[16] A. Theumer, C. Grafe, F. Bahring, et al., J. Magn. Magn. Mater. 380 (2015) 27–33.
[17] I. Canton, G. Battaglia, Chem. Soc. Rev. 41 (2012) 2718–2739.
[18] F.C. Perez-Martinez, J. Guerra, I. Posadas, et al., Pharm. Res. 28 (2011) 1843–1858.
[19] N.M. Zaki, N. Tirelli, Expert Opin. Drug Deliv. 7 (2010) 895–913.
[20] G.J. Doherty, H.T. McMahon, Annu. Rev. Biochem. 78 (2009) 857–902.
[21] T.G. Iversen, T. Skotland, K. Sandvig, Nano Today 6 (2011) 176–185.
[22] S.K. Balasubramanian, J. Jittiwat, J. Manikandan, et al., Biomaterials 31 (2010) 2034–2042.
[23] J.M. Rosenholm, V. Mamaeva, C. Sahlgren, et al., Nanomedicine 7 (2012) 111–120.
[24] K. Li, C. Chen, C. Chen, et al., Enzym. Microb. Technol. 72 (2015) 72–78.
[25] L. Qi, X. Lv, T. Zhang, et al., Sci. Rep. 6 (2016) 26961.
[26] S. Barber-Zucker, N. Keren-Khadmy, R. Zarivach, Protein Sci. 25 (2016) 338–351.
[27] B.H. Lower, D.A. Bazylinski, J. Mol. Microbiol. Biotechnol. 23 (2013) 63–80.
[28] K.T. Thurn, H. Arora, T. Paunesku, et al., Nanomedicine 7 (2011) 123–130.
[29] A. Ros-Baro, C. Lopez-Iglesias, S. Peiro, et al., Proc. Natl. Acad. Sci. USA 98 (2001) 12050–12055.
[30] K. Sarkar, M.J. Kruhlak, S.L. Erlandsen, et al., Immunology 116 (2005) 513–524.
[31] O. Lunov, V. Zablotskii, T. Syrovets, et al., Biomaterials 32 (2011) 547–555.
[32] J.A. Swanson, Nat. Rev. Mol. Cell Biol. 9 (2008) 639–649.